



A pulse stretcher for a LINAC-based pulsed slow-positron beam providing a quasi-continuous beam with an energy of 5.2 keV

K. Wada ^{a,b,*}, M. Maekawa ^a, I. Mochizuki ^b, T. Shidara ^c, A. Kawasuso ^a, M. Kimura ^b, T. Hyodo ^b

^a Takasaki Advanced Radiation Research Institute, Quantum Beam Science Research Directorate, National Institutes for Quantum and Radiological Science and Technology, 1233 Watanuki, Takasaki, Gunma 370-1292, Japan

^b Institute of Materials Structure Science, High Energy Accelerator Research Organization (KEK), 1-1 Oho, Tsukuba 305-0801, Japan

^c Accelerator Laboratory, High Energy Accelerator Research Organization (KEK), 1-1 Oho, Tsukuba 305-0801, Japan

ARTICLE INFO

Keywords:

Positron
Slow-positron beam
Positron annihilation
Low-energy positron diffraction (LEPD)

ABSTRACT

A pulse stretcher providing a 5.2 keV quasi-continuous beam has been developed for use with a pulsed slow-positron beam generated by an electron linear accelerator operated with a repetition frequency of 50 Hz. Pulses of positrons, of width 1.2 μs, were trapped in a Penning–Malmberg trap and then gradually released downstream, stretching the pulse width to nearly 20 ms.

1. Introduction

At the Institute of Materials Structure Science of High Energy Accelerator Research Organization (KEK), a high-intensity slow-positron beam is supplied from a normal-conducting electron linear accelerator (linac) via positron–electron pair creation. The system provides a pulsed slow-positron beam with an energy of 0.1 keV – 35 keV and is used for basic and materials science [1].

Recently, we have been developing a system for low-energy positron diffraction (LEPD), the positron counterpart of low-energy electron diffraction (LEED). The LEED/LEPD method is one in which a low-energy electron/positron beam is perpendicularly incident on a sample surface through the center hole of the detector and the diffraction pattern formed by backscattering is observed. Unlike the small electron gun of LEED, the large transportation system and geometrical conflicts of the positron beam apparatus pose difficulties in using an optical camera to record diffraction patterns from the back. Therefore, a two-dimensional position sensitive detector is needed, such as a delay-line detector (DLD) [2] or a resistive anode encoder (RAE) [3].

The intense pulsed beams generated with a linac are not, however, suitable for these counting detectors because of the signal pile-up in the detection system. For example, the long-pulse mode of the linac used, in which the maximum beam intensity is available, provides 10^6 slow- e^+ in every 1.2 μs pulse. This amounts to a positron density per unit time of 10^{12} slow- e^+ /s, which could lead to pile-up problems. In order to circumvent this issue whilst taking advantage of the high-intensity beam produced by the linac-based method, a pulse stretcher has been developed and incorporated into the system.

Attempts to construct pulse stretchers have been made at several facilities [4–8] for conventional positron annihilation γ -ray spectroscopies, which also have similar pile-up problems to linac-based pulsed beams. These stretchers first confine pulsed positrons in a Penning–Malmberg trap [9] and then release them gradually by decreasing the electrostatic potential of the exit electrode before the next pulse arrives. The energy of the output beam of these stretchers is low, typically 10 eV – 25 eV.

Another way of stretching linac-based positron pulses has also been attempted, in which a pulse of positrons is held in a Penning–Malmberg trap, and the trap potential is slowly raised while the exit potential is maintained at a fixed value lower than the entrance potential, so that the positrons with the highest kinetic energy within the trap spill over the exit electrode. The concept of this technique was proposed by the slow-positron group at Lawrence Livermore National Laboratory (LLNL) [10,11]. With this method, they released positrons from the trap with an energy of 20 eV and used them to obtain two-dimensional angular correlation of the annihilation radiation (2D-ACAR) spectra [12]. Also mentioned in this work was that this technique would provide a significantly-reduced energy-distribution of the quasi-continuous beam, making the bunching in a re-pulsing system downstream efficient for positron lifetime experiments.

In the present study, we followed the principle of the LLNL group, developing a new pulse stretcher which gives a quasi-continuous beam with an energy of up to 5.2 keV against the ground potential. A beam of ~ 5 keV maximizes the forward-reemission yield for a transmission-type remoderator [13,14] of Ni film with a thickness of ~ 150 nm [15] and W film with a thickness of ~ 100 nm [13]. In the present setup, the

* Corresponding author at: Institute of Materials Structure Science, High Energy Accelerator Research Organization (KEK), 1-1 Oho, Tsukuba 305-0801, Japan.
E-mail address: kenwada@post.kek.jp (K. Wada).

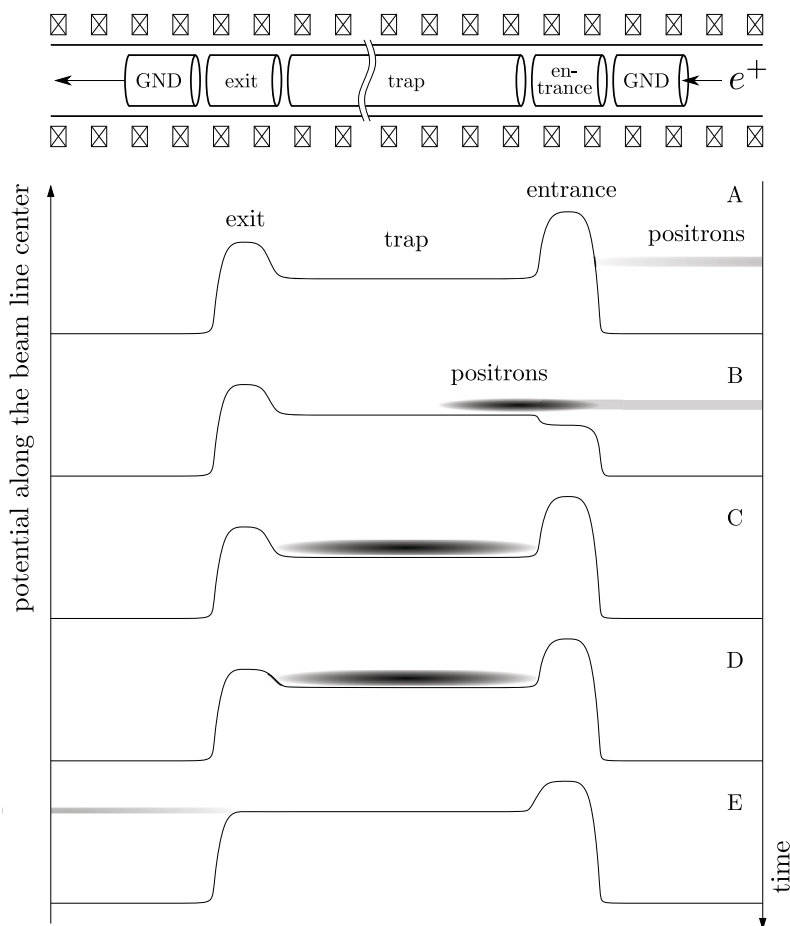


Fig. 1. A conceptual image of the pulse stretcher developed at KEK. Slow-positron pulses, coming from the right, are decelerated and confined in a Penning–Malmberg trap, and then released downstream slowly by raising the trap potential.

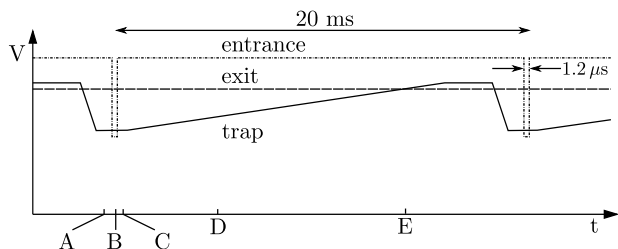


Fig. 2. An example of the temporal change in the potential of each electrode of the trap for the pulse stretching. The spatial distribution of the potential along the beam line center at the moment indicated by the letters A, B, ..., E in this figure are shown in Fig. 1.

resulting high-energy quasi-continuous beam was remoderated with a Ni film and used for LEPD experiments at the ground potential [16].

2. Experimental setup

A schematic diagram of the KEK slow-positron facility is shown in Ref. [16]. The linac is operated at ~ 50 MeV, < 0.6 kW with a repetition frequency of 50 Hz. Accelerated electrons are impinged on 4 mm thick Ta (converter) as shown in Figs. 1 and 2 of Ref. [1]. The electrons deflected by Ta nuclei emit Bremsstrahlung X-rays, causing positron-electron pair creation in the converter. A proportion of the high-energy positrons created is then thermalized in 25 μm thick W films (moderator) situated beside the converter and emitted with an energy corresponding to the negative work function for the positron, ~ 3 eV,

from the film surfaces. A voltage of 5.0 kV is applied to the converter. The two sets of moderators and the extraction grid beside the converter are subjected to a bias voltage of -10 V relative to each other. The moderated positrons are then accelerated to ~ 5.0 keV toward another grid at the entrance of the beam line at the ground potential and transported along a magnetic field to the experimental stations. The present pulse stretcher is located in the middle of the long straight beam line, upstream of the first-branching point leading the beam to the floor above.

A conceptual image of the present pulse stretcher is shown in Fig. 1. A grounded electrode, an entrance gate electrode, a ~ 6 m long trap electrode, an exit electrode, and another grounded electrode, which are all cylindrical, were situated inside the vacuum tube of the beam line. Positron pulses are trapped between the entrance and the exit electrodes, confined axially by electrostatic potentials and radially along the beam line by a magnetic field generated by coils.

The space-length of a slow-positron pulse of a certain time-width varies with its kinetic energy, becoming longer as the energy increases. For example, the space-length of a $1.2 \mu\text{m}$ pulse with an energy of 5 keV is ~ 50 m. Such a length is too long for this facility to accommodate in a linear trap, therefore the kinetic energy in the trapping section needs to be appropriately reduced. We constructed a Penning–Malmberg trap with a trap electrode of ~ 6 m long. A round-trip length of 12 m corresponds to the space-length of a $1.2 \mu\text{s}$ pulse with an energy of ~ 300 eV. During operation, the entrance gate electrode is normally kept at a higher potential than that at the exit electrode (Fig. 1 A). When a positron pulse arrives, the potential of the entrance gate electrode is temporarily lowered to allow entry into the trap electrode (Fig. 1 B). The positrons are decelerated on entering the entrance gate electrode,

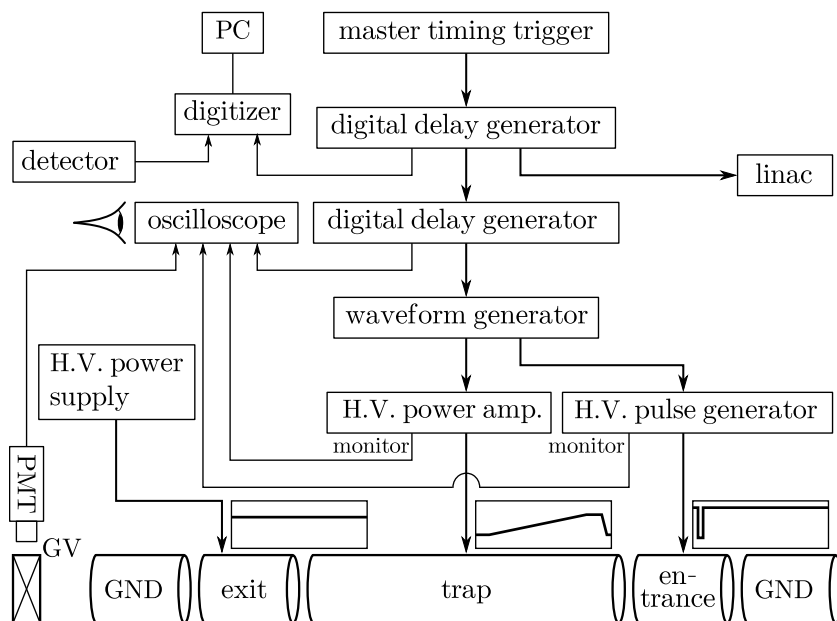


Fig. 3. Diagram of the timing circuit for the present pulse stretcher.

and decelerated further to be less than 300 eV when they reach the trap electrode. Positrons then travel along a solenoid magnetic field down to and are reflected back from the exit electrode, which is kept at a constant potential for the energy of outgoing positrons. The entrance electrode potential is raised back to the initial value before the positrons return in 1.2 μs , in order to prevent escape (Fig. 1 C). The trap electrode potential is then increased gradually, letting the positrons spill over the exit electrode with a fixed kinetic energy set by the potential of the exit electrode (Fig. 1 D to E).

This system allows positrons in the trap to pass through the exit electrode in order of highest kinetic energy first. By adjusting the sweeping speed of the trapping electrode potential, we can vary the width of the stretched pulse beam up to the pulse interval, 20 ms, which makes an almost a continuous beam. An example of the temporal change of the potential at the three electrodes is given in Fig. 2.

A diagram of the timing circuit for the pulse stretcher is shown in Fig. 3. A timing signal generated by the master timing trigger is branched by the first digital delay-generator. One of the branched signal triggers the linac, while a second triggers a waveform generator (Tektronix AFG3022C) and a digital oscilloscope through a second digital delay-generator (SRS DG535). The waveform generator drives the high-voltage pulse generator (DEI PVX-4130) and the high-voltage power amplifier (Matsusada Precision HEOPT-20B10) to control the potentials at the entrance and the trap electrodes, respectively. The digital oscilloscope monitors the potential supplied to the entrance and trap electrodes together with the signal from an annihilation γ -ray detector. This detector is placed close to a gate valve downstream of the pulse stretcher in order to observe the beam. The third signal from the first digital delay-generator is fed to the experimental station and is used to synchronize the detection system with the operation of the pulse stretcher.

Fig. 4 shows a cross-section of the electrodes, vacuum tubes, and trapping/transporting coils around the entrance electrode. The corresponding part around the exit electrode is symmetrical with this figure. The grounded electrodes are 75 mm long with an inner diameter of 58 mm. The entrance and exit electrodes are 160 mm long with the same inner diameter. The trap electrode is 5780 mm long with an inner diameter of 69 mm. The gap between the ground and the entrance/exit electrode is 4 mm, and that between the trap and the entrance/exit electrodes is 2 mm. The coils for the Penning–Malmberg trap are polyester enameled wires 2 mm in diameter wound 300 turns on a spool-type

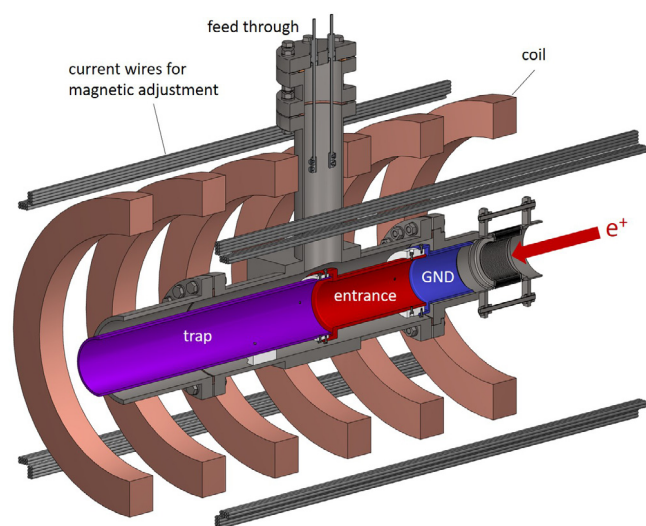


Fig. 4. A schematic diagram around the entrance electrode of the Penning–Malmberg trap. A cross-sectional view of the electrodes, vacuum tubes, and trapping/transporting magnetic coils, together with current wiring for magnetic field adjustment, are shown.

frame with a dimension of $\phi 310 \text{ mm} \times 40 \text{ mm}$. These coils are arranged 125 mm apart between the centers. With a current of 6.5 A, a magnetic field of $\sim 15 \text{ mT}$ can be generated along the beam line center. A typical magnetic field during the operation of the pulse stretcher is $\sim 10 \text{ mT}$. The earth's magnetic field is adequately compensated for using long rectangular coils consisting of 8 turns of wires surrounding the whole pulse stretcher, connected to $\pm 5 \text{ A}$ bipolar current sources. Parts of these coils are also shown in Fig. 4.

A calculated electrostatic potential around the exit electrode is shown in Fig. 5(a), where r is the radial distance from the center line of the electrodes, and z is a coordinate along the center line. A contour plot shows the electrostatic potential from 4735 V to 5190 V at 35 V intervals when potentials of 4740 V and 5200 V are applied to the trap and the exit electrode, respectively. The potential along the center of the beam line is plotted in Fig. 5(b). Values of the difference in potential at $r = 10 \text{ mm}$ and $r = 0 \text{ mm}$ and that at $r = 5 \text{ mm}$ and $r = 0 \text{ mm}$

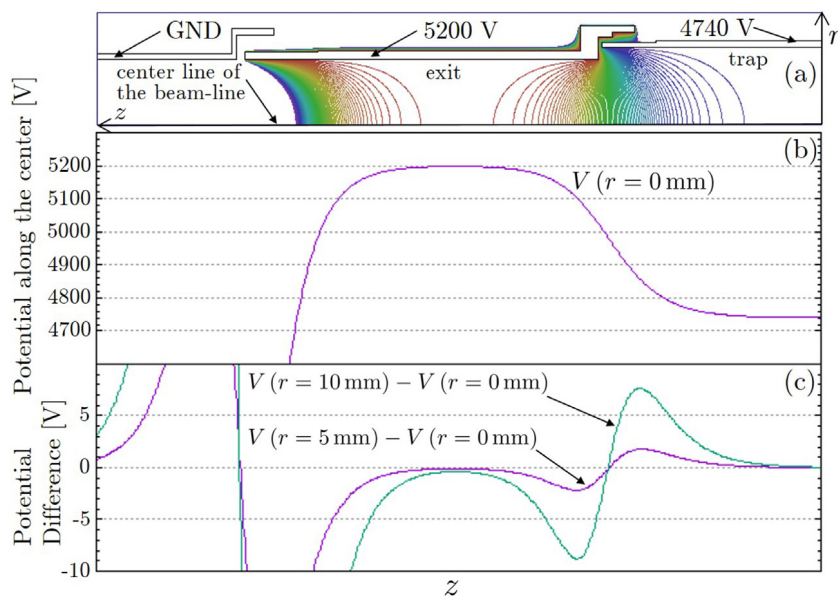


Fig. 5. An example of a calculated electrostatic potential around the exit electrode, where r is the radial distance from the center line and z is a coordinate along the center line. (a) Contour plot showing electrostatic potential from 4735 V to 5190 V at 35 V intervals when potentials of 4740 V and 5200 V are applied to the trap and the exit electrode, respectively. (b) The potential along the center of the beam line, $V(r=0\text{ mm})$. (c) The difference in potential at $r=10\text{ mm}$ and $r=0\text{ mm}$ ($V(r=10\text{ mm}) - V(r=0\text{ mm})$), and that at $r=5\text{ mm}$ and $r=0\text{ mm}$ ($V(r=5\text{ mm}) - V(r=0\text{ mm})$).

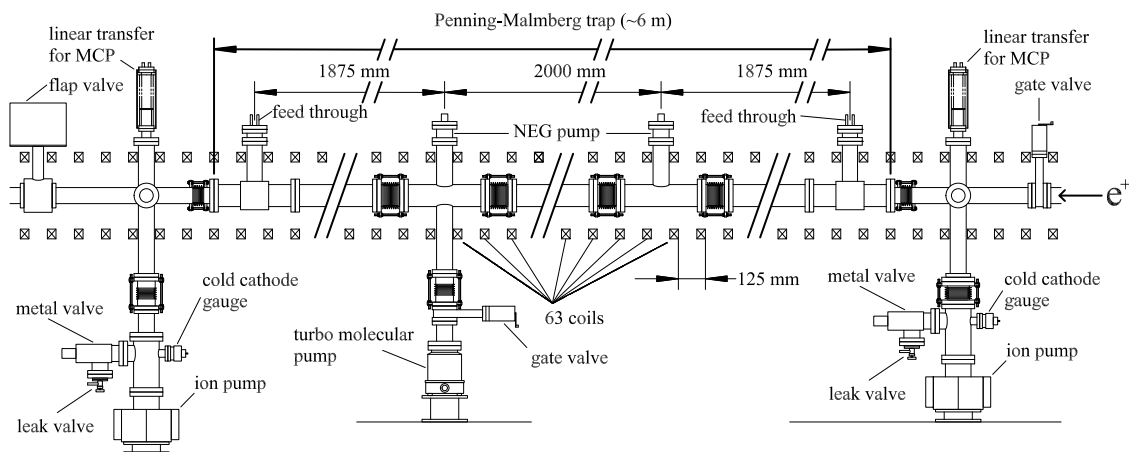


Fig. 6. Layout of the vacuum system for the present pulse stretcher. Long parts are partially omitted in this figure. “NEG pump” denotes non-evaporable getter pump.

with respect to z are plotted in Fig. 5(c). Within the exit electrode, the minimum value of the former difference is 0.4 V, and that of the latter difference is 0.1 V. This shows that the difference in the potential barrier at the exit electrode experienced by the positrons with a beam radius of 5 mm (the half width at tenth maximum (HWTM) of the beam intensity) is expected to be constant within $\sim 100\text{ mV}$.

A layout of the vacuum system for the present pulse stretcher is shown in Fig. 6 (long parts partially omitted). Two non-evaporable getter (NEG) pumps (SAES CapaciTorr D1000), two ion pumps (Varian (Agilent) Vaclon Plus 75 StarCell), and a turbo molecular pump (Edwards STP-301) were installed. Two holes of dimension 60 mm and 52 mm were made in the trap electrode, opening to the NEG pumps through 20 wires/inch meshes. A gate valve on the turbo molecular pump was open during the baking of the beam line and closed after cool-down to room temperature. Following a one-week bake-out and activation of the NEG pumps, two cold cathode gauges placed outside the coils measured the pressure to be $\sim 1 \times 10^{-7}\text{ Pa}$ with current flow through the coils (whereupon an accompanying slight temperature rise of the beam-line was noted). A fast-closing isolation flap-valve was installed downstream of the pulse stretcher to protect the upstream side

including the slow-positron production unit and the linac. Its function was to close automatically within a few tens of ms on detection of a pressure rise in an emergency such as an unintended vacuum leak. Electrical feedthroughs were installed at both ends of the trap to apply potential to the electrodes (also shown in Fig. 4). Linear transfers, to which an assembly of multi-channel plates (MCP) and a fluorescent screen were attached, were installed upstream and downstream of the pulse stretcher to monitor the beam.

3. Results and discussion

We confirmed that the initial $1.2\text{ }\mu\text{s}$ pulse was extended in width from about $200\text{ }\mu\text{s}$ to nearly 20 ms with the present system. The lower limit of the stretched pulse width is due to the bandwidth of the high-voltage amplifier connected to the capacitive trap electrode, and the upper limit is simply the interval of 50 Hz pulses.

Fig. 7 shows an example of pulse stretching to a width of 15 ms with the present system. Fig. 7(a) represents the monitor output of the high-voltage power amplifier, which supplied a varying potential to the trap electrode. It was observed using a digital oscilloscope in the AC

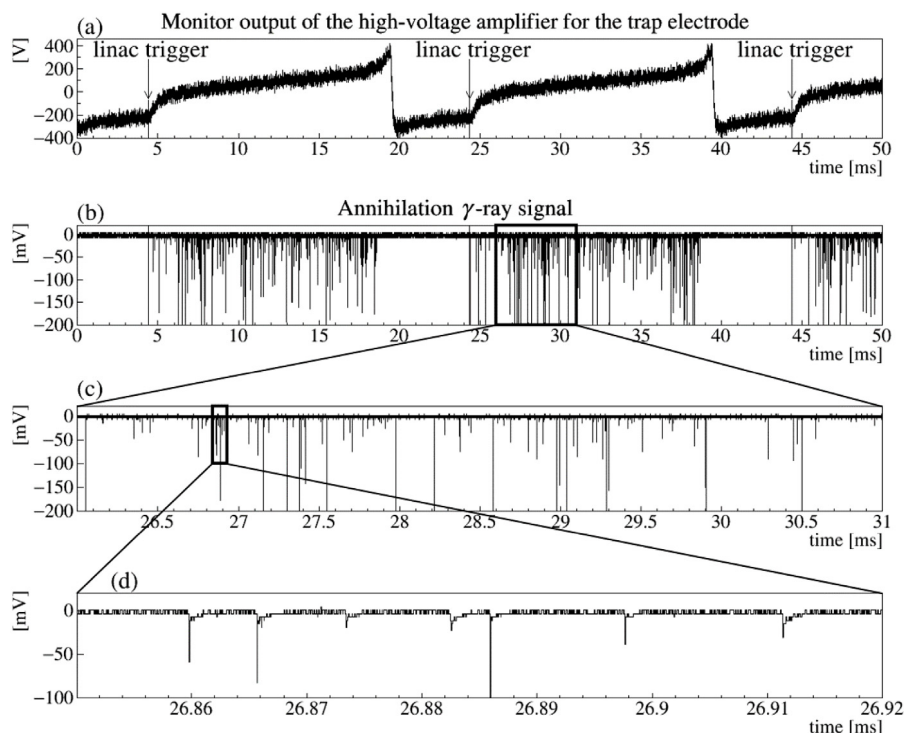


Fig. 7. An example of the performance of the present pulse stretcher with 15 ms pulse stretching. (a) Monitor output of the high-voltage power amplifier, which supplied a varying potential to the trap electrode. It was observed using a digital oscilloscope in the AC coupling mode, so that the vertical axis of the plot shows the relative variation from the DC component. The output was actually varied from 4.8 kV to 5.4 kV, synchronized with the linac trigger at a rate of 50 Hz. (b) Annihilation γ -ray signal due to positrons that passed through the exit electrode kept at 5.2 kV and annihilated upon reaching the closed gate valve downstream. Signals were detected by a plastic scintillator mounted on a photomultiplier tube (PMT), which was placed nearby. (c), (d) Enlarged views of the area denoted by the boxes in (b) and (c), respectively.

coupling mode, so that the vertical axis of the plot shows the relative variation from the DC component. The output was actually varied from 4.8 kV to 5.4 kV, synchronized with the linac trigger at a rate of 50 Hz. The amplifier was driven by the waveform generator. The waveform in this case was adjusted to give a flat intensity from an assumed Gaussian energy distribution of the incoming pulse. Fig. 7(b) shows annihilation γ -ray signals detected by a plastic scintillator mounted on a photomultiplier tube (PMT), which was placed downstream near the closed gate valve where the positrons annihilated. The signals were observed only while the trap potential was gradually increased, showing that the initial pulses of width $1.2 \mu\text{s}$ were stretched to $\sim 15 \text{ms}$. Fig. 7(c) is an enlarged view of the area denoted by the box in (b), and Fig. 7(d) is a further enlarged view of the box area in (c). Each individual annihilation- γ is distinguished in (d).

Fig. 8(a) and (b) show typical images of the slow-positron beam on a MCP/phosphor-screen assembly observed downstream of the pulse stretcher without and with the pulse stretcher operation, respectively. The elliptical beam shape became circular when the pulse stretcher was initiated. The visible beam diameter was $\sim 10 \text{mm}$.

Fig. 9(a) shows the positrons remaining after trapping for various storage times. Fig. 9(c) shows profiles of the ramping trap potential, A to H, increasing linearly from 4.56 kV to 5.4 kV, where the starting time increases stepwise. One ramp corresponds to an independent run for one pulse but ramps are depicted here as overlapping. Fig. 9(b) shows the intensity profile of the annihilation γ -ray signals observed downstream corresponding to each delayed ramp of the potential. The time dependence of the relative intensity shown in (a) is normalized to the “time zero” value, which was estimated by the extrapolation of the intensities to the trap start time. From the result, it was estimated that the half-life of the intensity was 85 ms or a 15% loss after 20 ms confinement.

The vacuum level is crucially important for the storage of positrons. Previous experiments have shown that 95% of the positrons remained for 1 ms in a vacuum of 10^{-6}Pa but all of the positrons were lost in the

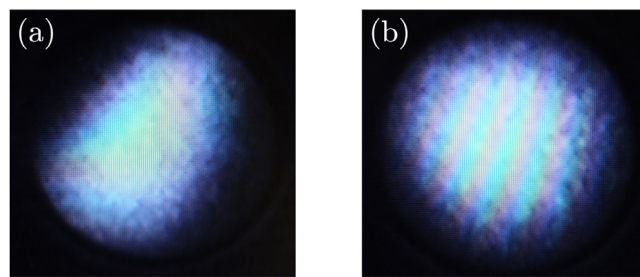


Fig. 8. Typical images of the slow-positron beam on a MCP/phosphor-screen assembly (a) without and (b) with the pulse stretcher operation. The visible beam diameter is $\sim 10 \text{mm}$.

same confinement time in a vacuum of 10^{-4}Pa [7,8]. The result in Fig. 9 indicates that 99% of the positrons remained during trapping over 1 ms in a vacuum of 10^{-7}Pa with the present system, which corresponds to a 5-times longer trap life-time than that observed at 10^{-6}Pa , as previously reported. The longer trap life-time observed was thought to be attained due to better vacuum conditions.

The present pulse stretcher has been incorporated into a low-energy positron diffraction (LEPD) system with a transmission type remoderator, which has succeeded in observing LEPD patterns detected by a DLD [16]. We have enhanced the brightness of the stretched pulse beam with a remoderator of 150 nm thick Ni film, and used the remoderated beam in the grounded LEPD experiment chamber. The present pulse stretcher has resolved the multi-hit problem which features in the counting-based system.

In Figs. 7 and 9, and in the actual LEPD measurements [16], the positron energy was raised by about 200 eV, leading to a mono-energetic beam with an energy of 5.2 keV after pulse stretching. With the present system, the energy of the output positrons can be set, in

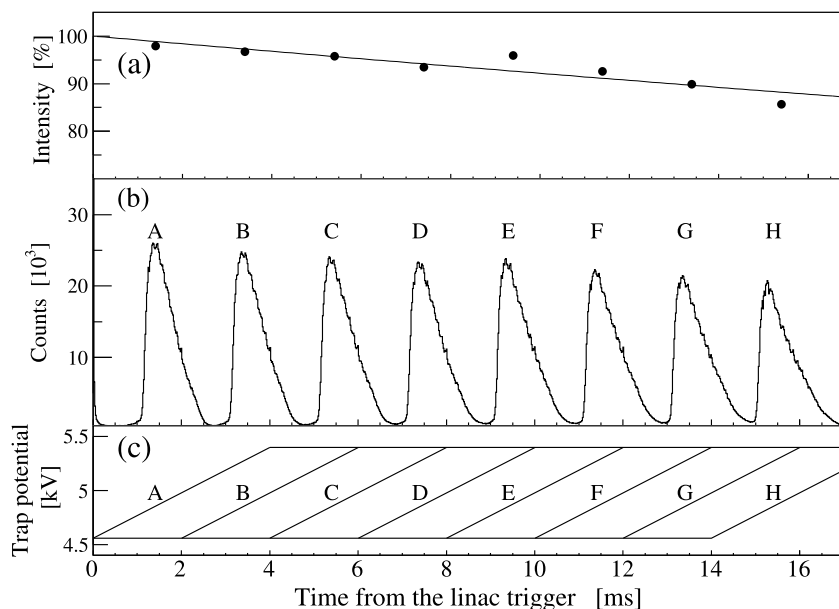


Fig. 9. (a) Percentage decrease in the positron intensity during trapping with the present Penning–Malmberg trap. The relative intensities were observed by storing positrons for different confinement times then released by the ramping profiles of the trap potential shown in (c). (b) Total count of annihilation γ -rays detected downstream.

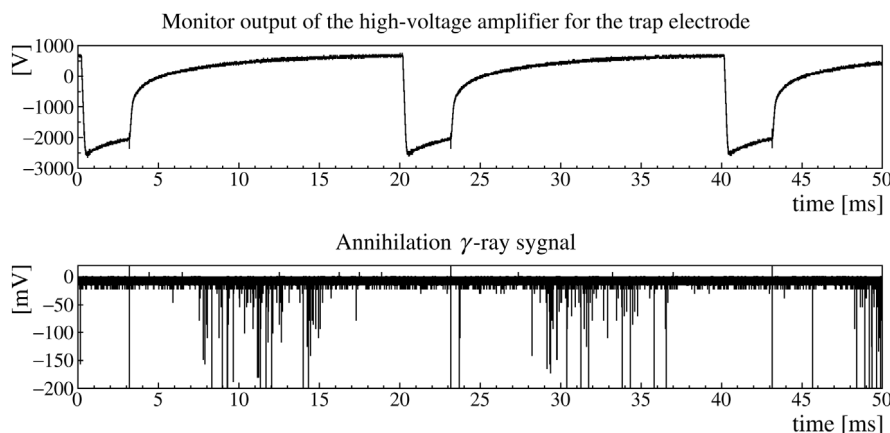


Fig. 10. An example of the energy elevation of the positron beam from 2.7 keV to 5.2 keV. The top plot represents the monitor output of the high-voltage power amplifier, which supplied a varying potential to the trap electrode, observed using a digital oscilloscope in the AC coupling mode. The output of the amplifier was actually varied from 2.44 kV to 5.4 kV. The bottom plot shows annihilation γ -ray signals due to positrons going through the exit electrode at 5.2 keV and annihilating at a closed gate valve downstream.

principle, at any value higher than the initial energy of the positrons, i.e., it has the function of an energy elevator. Fig. 10 shows an example of another energy elevation; an initial energy of 2.7 keV is elevated to an output energy of 5.2 keV. The top plot represents the monitor output of the high-voltage amplifier, which supplied a varying potential to the trap electrode, observed using a digital oscilloscope in the AC coupling mode. The output of the amplifier was actually varied from 2.44 kV to 5.4 kV. The exit electrode potential was set at 5.2 kV. The γ -ray signal from the output positrons hitting the closed gate valve downstream is shown in the lower plot. An increase in energy from less than 2.7 keV or to that greater than 5.4 keV was not possible due to discharge between the electrodes. However, it should be possible to suppress the discharge by introducing more gaps between the electrodes.

4. Conclusion

A pulse stretcher with a Penning–Malmberg trap has been developed for a linac-based pulsed slow-positron beam with an energy of ~ 5 keV. The initial beam with a pulse width of $1.2 \mu\text{s}$ has been stretched to nearly 20 ms, which is the interval of 50 Hz pulses. It has been incorporated into a low-energy positron diffraction (LEPD) system with a

transmission type remoderator. The issue of possible pile-up in the detection system, synonymous with the use of intense pulsed beam, has been resolved. With this system, LEPD patterns were successfully observed in a grounded chamber. Furthermore, we have demonstrated an energy elevation of a positron beam with an initial energy of 2.7 keV to an energy of 5.2 keV with this system. Further energy elevation should be possible by introducing larger gaps between the electrodes of the trap to suppress discharge.

CRediT authorship contribution statement

K. Wada: Formal analysis, Funding acquisition, Methodology, Software, Writing - original draft. **M. Maekawa:** Conceptualization, Visualization. **I. Mochizuki:** Investigation, Methodology, Validation. **T. Shidara:** Resources, Writing - review & editing. **A. Kawasuso:** Supervision, Writing - review & editing. **M. Kimura:** Funding acquisition, Writing - review & editing. **T. Hyodo:** Funding acquisition, Project administration, Writing - review & editing.

Declaration of competing interest

The authors declare that they have no known competing financial interests or personal relationships that could have appeared to influence the work reported in this paper.

Acknowledgment

We appreciate the discussions with Dr. R. H. Howell on the pulse stretching system. This work was supported by Toray Science and Technology Grant, the Cross Ministerial Strategic Innovation Promotion Program (SIP, unit D66), JSPS KAKENHI Grant Numbers JP24221007 and JP18H03476. Experiments were conducted under the approval of the PF PAC (Proposal Nos. 2014G636, 2015S2-002, 2016S2-001, 2016S2-006) and under the auspices of the QST-KEK Joint Development Research.

References

- [1] K. Wada, T. Hyodo, A. Yagishita, M. Ikeda, S. Ohsawa, T. Shidara, K. Michishio, T. Tachibana, Y. Nagashima, Y. Fukaya, M. Maekawa, A. Kawasuso, Increase in the beam intensity of the linac-based slow positron beam and its application at the slow positron facility, KEK, *Eur. Phys. J. D* 66 (2012) 37–1–4, <http://dx.doi.org/10.1140/epjd/e2012-20641-4>.
- [2] O. Jagutzki, V. Mergel, K. Ullmann-Pfleger, L. Spielberger, U. Spillmann, R. Dörner, H. Schmidt-Böcking, A broad-application microchannel-plate detector system for advanced particle or photon detection tasks: large area imaging, precise multi-hit timing information and high detection rate, *Nucl. Instrum. Methods Phys. Res. A* 477 (2002) 244–249, [http://dx.doi.org/10.1016/S0168-9002\(01\)01839-3](http://dx.doi.org/10.1016/S0168-9002(01)01839-3).
- [3] M. Lampton, F. Paresce, The ranicon: A resistive anode image converter, *Rev. Sci. Instrum.* 45 (1974) 1098–1105, <http://dx.doi.org/10.1063/1.1686818>.
- [4] L.D. Hulet Jr., T.A. Lewis, R.G. Alsmiller Jr., R. Peelle, S. Pendyala, J.M. Dale, T.M. Rosseel, A design for a high intensity slow positron facility using forward scattered radiation from an electron linear accelerator, *Nucl. Instrum. Methods Phys. Res. B* 24 (1987) 905–908, [http://dx.doi.org/10.1016/S0168-583X\(87\)80276-8](http://dx.doi.org/10.1016/S0168-583X(87)80276-8).
- [5] Y. Ito, O. Sueoka, M. Hirose, M. Hasegawa, S. Takamura, T. Hyodo, Y. Yabata, Production of intense positron beam using 100 mev linac, in: L. Dorikens-Vanpraet, M. Dorikens, D. Segers (Eds.), *Proc. 8th Int. Conf. Positron Annihilation*, World Scientific, 1989, pp. 583–585.
- [6] T. Akahane, T. Chiba, N. Shiotani, S. Tanigawa, T. Mikado, R. Suzuki, M. Chiwaki, T. Yamazaki, T. Tomimasu, Stretching of slow positron pulses generated with an electron linac, *Appl. Phys. A* 51 (1990) 146–150, <http://dx.doi.org/10.1007/BF00324279>.
- [7] J. Paridaens, D. Segers, M. Dorikens, L. Dorikens-Vanpraet, Pulse stretching at the linac-based slow-positron beam of the ghent university, *Nucl. Instrum. Methods Phys. Res. A* 295 (1990) 39–43, [http://dx.doi.org/10.1016/0168-9002\(90\)90419-7](http://dx.doi.org/10.1016/0168-9002(90)90419-7).
- [8] D. Segers, J. Paridaens, M. Dorikens, L. Dorikens-Vanpraet, Beam handling with a penning trap of a linac-based slow positron beam, *Nucl. Instrum. Methods Phys. Res. A* 337 (1994) 246–252, [http://dx.doi.org/10.1016/0168-9002\(94\)91091-X](http://dx.doi.org/10.1016/0168-9002(94)91091-X).
- [9] J.H. Malmberg, C.F. Driscoll, Long-time containment of a pure electron plasma, *Phys. Rev. Lett.* 44 (10) (1980) 654–657, <http://dx.doi.org/10.1103/PhysRevLett.44.654>.
- [10] R.H. Howell, W. Stoeffl, A. Kumar, P.A. Sterne, T.E. Cowan, J. Hartley, High current pulsed positron microprobe, *Mater. Sci. Forum* 255–257 (1997) 644–646, <http://dx.doi.org/10.4028/www.scientific.net/MSF.255-257.644>.
- [11] W. Stoeffl, P. Asoka-Kumar, R. Howell, The positron microprobe at LLNL, *Appl. Surf. Sci.* 149 (1999) 1–6, [http://dx.doi.org/10.1016/S0169-4332\(99\)00162-2](http://dx.doi.org/10.1016/S0169-4332(99)00162-2).
- [12] T. Gessmann, M. Petkov, M.H. Weber, K.G. Lynn, K.P. Rodbell, P. Asoka-Kumar, W. Stoeffl, R.H. Howell, Study of positronium in low-k dielectric films by means of 2D-angular correlation experiments at a high-intensity slow-positron beam, *Mater. Sci. Forum* 363–365 (2001) 585–587, <http://dx.doi.org/10.4028/www.scientific.net/MSF.363-365.585>.
- [13] D.M. Chen, K.G. Lynn, R. Pareja, B. Nielsen, Measurement of positron reemission from thin single-crystal W(100) films, *Phys. Rev. B* 31 (1985) 4123–4130, <http://dx.doi.org/10.1103/PhysRevB.31.4123>.
- [14] N. Zafar, J. Chevallier, G. Laricchia, M. Charlton, Single-crystal nickel foils as positron transmission-mode moderators, *J. Phys. D: Appl. Phys.* 22 (1989) 868–870, <http://dx.doi.org/10.1088/0022-3727/22/6/031>.
- [15] M. Fujinami, S. Jinno, M. Fukuzumi, T. Kawaguchi, K. Oguma, T. Akahane, Production of a positron microprobe using a transmission remoderator, *Anal. Sci.* 24 (2008) 73–79, <http://dx.doi.org/10.2116/analsci.24.73>.
- [16] K. Wada, T. Shirasawa, I. Mochizuki, M. Fujinami, M. Maekawa, A. Kawasuso, T. Takahashi, T. Hyodo, Observation of low-energy positron diffraction patterns with a linac-based slow-positron beam, *e-J. Surf. Sci. Nanotechnol.* 16 (2018) 313–319, <http://dx.doi.org/10.1380/ejsnt.2018.313>.